2 mip

NASA TECHNICAL NOTE

NASA TN D-7561

NASA TN D-7561

COLLISIONLESS RELAXATION IN SPIRAL GALAXY MODELS

by Frank Hohl

Langley Research Center
Hampton, Va. 23665

NATIONAL AERONAUTICS AND SPACE ADMINISTRATION • WASHINGTON, D. C. • JUNE 1974

1. Report No.	2. Government Accession No.	3. Recipient's Catalog No.
NASA TN D-7561		

4. Title and Subtitle	5. Report Date
COLLISIONLESS RELAXATION IN SPIRAL GALAXY MODELS	June 1974
	6. Performing Organization Code
7. Author(s)	8. Performing Organization Report No.
Frank Hohl	L-9385
	10. Work Unit No.
9. Performing Organization Name and Address	188-41-51-01
NASA Langley Research Center Hampton, Va. 23665	11. Contract or Grant No.
	13. Type of Report and Period Covered
12. Sponsoring Agency Name and Address	Technical Note
National Aeronautics and Space Administration Washington, D.C. 20546	14. Sponsoring Agency Code

15. Supplementary Notes

16. Abstract

The increase in random kinetic energy of stars by rapidly fluctuating gravitational fields (collisionless or violent relaxation) in disk galaxy models is investigated for three interaction potentials of the stars corresponding to (a) point stars, (b) rod stars of length 2 kpc, and (c) uniform density spherical stars of radius 2 kpc. To stabilize the galaxy against the large-scale bar-forming instability, a fixed field corresponding to a central core or halo component of stars was added with the stars containing at most 20 percent of the total mass of the galaxy. Considerable heating occurred for both the point stars and the rod stars, whereas the use of spherical stars resulted in a very low heating rate. The use of spherical stars with the resulting low heating rate will be desirable for the study of large-scale galactic stability or density wave propagation, since collective heating effects will no longer mask the phenomena under study.

17. Key Words (Suggested by Author(s))	18. Distribution Statement
Spiral galaxy models Computer simulation	Unclassified – Unlimited STAR Category 30

19. Security Classif. (of this report)	20. Security Classif. (of this page)	21. No. of Pages	22. Price*
Unclassified	Unclassified	21	$3.00

*For sale by the National Technical Information Service, Springfield, Virginia 22151

COLLISIONLESS RELAXATION IN SPIRAL GALAXY MODELS

By Frank Hohl
Langley Research Center

SUMMARY

The increase in random kinetic energy of stars by rapidly fluctuating gravitational fields (collisionless or violent relaxation) in disk galaxy models is investigated for three interaction potentials of the stars corresponding to (a) point stars, (b) rod stars of length 2 kpc, and (c) uniform-density spherical stars of radius 2 kpc. To stabilize the galaxy against the large-scale bar-forming instability, a fixed field corresponding to a central core or halo component of stars was added with the stars containing at most 20 percent of the total mass of the galaxy. Considerable heating occurred for both the point stars and the rod stars, whereas the use of spherical stars resulted in a very low heating rate. The use of spherical stars with the resulting low heating rate will be desirable for the study of large-scale galactic stability or density wave propagation, since collective heating effects will no longer mask the phenomena under study.

INTRODUCTION

Recent numerical simulations of the evolution of disk galaxies (ref. 1) show that the two-body relaxation time in these models is several hundred rotation periods. The large velocity dispersion acquired by stars in the large-scale N-body simulations (refs. 2 and 3) is therefore not a result of two-body relaxation or collisional effects. Thus, the increase in the velocity dispersion must be ascribed to heating by turbulent gravitational fields or violent relaxation as discussed by Lynden-Bell. (See ref. 4.) Since the time rate of change in total energy of a star $m\,d\left(V^2/2 - \phi\right)/dt$ is equal to the time rate of change in the gravitational field $-m(\partial\phi/\partial t)$, the acceleration or heating due to violent relaxation does not lead to mass segregation. The opposite holds for two-body relaxation or collisional effects which lead to equipartition of energy among stars of different mass. (See ref. 1.) Disks of stars that are stabilized in accordance with Toomre's (ref. 5) local criterion for axisymmetric stability are generally found to be unstable to the large-scale nonaxisymmetric bar-making instability. (See ref. 3.) The heating of stars due to collisionless relaxation can be investigated under more controlled conditions by adding an axisymmetric gravitational field to suppress the bar instability. In an actual galaxy this field could be supplied by the central core or halo population of stars. In this paper an

investigation is made of the collisionless relaxation of a disk of stars under the influence of a fixed field. The effects of softening the interaction potential of the stars on the heating rate are investigated by using the potential corresponding to finite-length mass rods and uniform-density spheres or spherical stars.

The model used for the calculations is that described earlier (ref. 6) with the fixed radial field added.

SYMBOLS

f	distribution function
G	gravitational constant
l	length of rod "stars"
$M_\odot$	solar mass, 1.989×10^{30} kg
m	mass
$Q = \frac{\sigma_r}{\sigma_{r,min}}$	
r	radial coordinate
r_s	radius of spherical "stars"
t	time
V	velocity, km/sec
κ	epicyclic frequency, km-sec^{-1}-kpc^{-1}
μ	surface mass density, $M_\odot$-kpc^{-2}
σ	velocity dispersion, km-sec^{-1}
$\sigma_{r,min} = 3.36G\mu/\kappa$, km-sec^{-1}	
ϕ	gravitational potential
Ω	angular velocity, km-sec^{-1}-kpc^{-1}

Subscripts:

min	minimum
r,θ	radial and azimuthal component

RESULTS

The fixed axisymmetric component of the gravitational field used in the first part of the calculations corresponds to a rotation curve (ref. 7) similar to the Schmidt model of the galaxy (ref. 8)

$$V_\theta = \frac{4600r}{100 + r^2} + \frac{210r}{0.25 + r^2} \text{ km/sec} \tag{1}$$

for values of r up to 30 kpc.

The 50 000 interacting stars used in the calculation move under the influence of this field and constitute about 20 percent of the total mass of the system. Three different interaction potentials of the stars were used in the calculations:

(1) Point stars

$$\phi_1(r) = \frac{Gm}{r}$$

(2) Rod stars of length 2 kpc

$$\phi_2(r) = Gm\left[\frac{r\left(1 - \sqrt{1 + \frac{4}{r^2}}\right)}{2} + \log_e\left(\frac{2}{r} + \sqrt{1 + \frac{4}{r^2}}\right)\right]$$

(3) Uniform-density spherical stars of radius 2 kpc

$$\phi_3(r) = \frac{Gm\left(3 - \frac{r^2}{4}\right)}{4} \qquad (r \leqq 2)$$

$$\phi_3(r) = \frac{Gm}{r} \qquad (r > 2)$$

Figure 1 illustrates these three potentials. Note that for $r \leqq 0.5$ kpc, the potential is constant so that the self force on a star is zero. For $r > 2$ kpc, the interactions are practically identical. The size of each of the $n \times n$ array of cells used in the self-consistent potential calculation is 0.5 kpc so that the modification of the potential extends

over four cell dimensions. Note that this modification of the potential is essentially an artificial means to reduce the short wavelength collective instabilities while the long range or global behavior remains essentially unchanged. For example, such an effect could be caused in real galaxies if a large fraction of the mass was in large interpenetrating gas clouds.

The evolution of the disk of 50 000 stars under the influence of the fixed radial field corresponding to the rotation curve of equation (1) is shown in figure 2. The fixed component of the gravitational field corresponds to 80 percent of the total system mass, the remaining 20 percent of the mass being contained in the stars. Three different systems are shown corresponding to the interaction potential used for each of the 50 000 stars in the disk: (a) point stars, (b) rod stars of length 2 kpc, and (c) spherical stars of radius 2 kpc. An initial velocity dispersion corresponding to Toomre's (ref. 5) local criterion for axisymmetric stability was given to the stars, that is,

$$\sigma_r = \sigma_{r,min} = 3.36 \frac{G\mu(r)}{\kappa(r)}$$

and

$$\sigma_\theta = \frac{\kappa(r)}{2\Omega(r)} \sigma_{r,min}$$

where G is the gravitational constant, $\mu(r)$ is the surface mass density of the stars, and $\kappa(r)$ is the epicyclic frequency including the effects of the fixed field plus stars. The initial mass density is given by $\mu(r) = \mu(0)\sqrt{1 - \frac{r^2}{R^2}}$ where R is the radius of the disk. The time shown in figure 2 and subsequent figures is in units of the rotation period at $r = 10$ kpc. The initial radius of the disk is 20 kpc. As can be seen, in all three cases a spiral structure develops and remains throughout the simulation period (5 rotations). The spiral structure extends toward the center of the disk to a radius of about 5 kpc. No spiral structure exists within this radius. Also, when the spirals first form, they rotate with essentially the same angular velocity as the stars, for example, 25 km-sec^{-1}-kpc^{-1} at a radius of 10 kpc. During the first two rotations the spiral elements are not fixed rotating structures. They have a tendency to diffuse or break in one region and then merge with other nearby components of spiral structure. This is the case especially in regions of high differential rotation (inner regions). Thus, the spiral structure is quite dynamic in reforming spiral arm components until after the first three rotations when there is a tendency to form a two-arm spiral structure. The spiral structure in this case is formed primarily by a combination of gravitational instability and differential rotation.

It is of interest to compare the rotation curves $\Omega(r)$ and epicyclic frequency $\kappa(r)$ for the three interaction potentials used. This comparison is made in figure 3. Also shown are the curves for $\Omega + \frac{\kappa}{2}$ and $\Omega - \frac{\kappa}{2}$ which are an indication of where spiral patterns can be the result of a density wave as proposed by Lin et al. (See ref. 9.) That is, for a constant spiral pattern speed Ω_S, a density wave is allowed only between the curves $\Omega + \frac{\kappa}{2}$ and $\Omega - \frac{\kappa}{2}$. Note that for low spiral pattern speeds ($\approx$15 km-sec^{-1}-kpc^{-1}) no density wave is allowed for small r, and no spiral structure is present for $r \lesssim 5$ kpc in figure 2. However, the "pattern speed" in figure 2 is only slightly less (at most 10 percent) than the mean rotation speed of the stars. Thus, the spiral structure cannot be considered a density wave. This result is in contrast to previous simulations without the background field where the pattern speed was considerably less than the rotation velocity of the stars (refs. 2 and 3).

To illustrate the heating rates for the three interaction potentials, figure 4 shows the evolution of

$$Q = \frac{\sigma_r(r,t)}{\sigma_{r,min}(r,t)}$$

the ratio of the radial velocity dispersion to that required by Toomre's criterion. The results show that for point stars Q quickly increases to a value near 2. For rod stars the values of Q are generally slightly less, especially in the inner regions of the disk. However, for the spherical stars, values of Q are only slightly above 1 over most of the disk. The rise in Q in the region from 15 to 20 kpc is due primarily to the reduction in the surface mass density as shown in figure 5. This condition effectively reduces $\sigma_{r,min}$ during the evolution of the system and results in a larger Q. Thus, the use of finite-size spherical stars effectively softens the interaction to give a slower heating rate and thus allows a cooler disk. The evolution of the actual radial velocity dispersion is shown in figure 6. Note that the radial velocity dispersion for the finite-size spherical stars shows only very little increase, the peak velocity remaining near 40 km/sec. At the same time σ_r for the point and rod stars increases to around 60 km/sec. More detailed information can be obtained from the radial velocity distribution of stars in different regions of the disk as shown in figure 7. Note the drastic decrease of the low-velocity stars in the central region ($r < 4$ kpc) of the disk for the point stars. In contrast for the spherical stars, the relaxation effects result in only a slight reduction of the low-velocity stars in that region. Thus, figure 7 illustrates again that for both the point and rod stars, there is considerable heating, whereas for the spherical stars heating occurs at a much lower rate. As expected, the same results were obtained for the azimuthal velocity distribution.

These calculations were repeated for a fixed field corresponding to a uniform-density spherical mass of radius 2 kpc. Therefore, for $r > 2$ kpc, the fixed field is Keplerian. Also, the 50 000 stars now contain only 10 percent of the total mass of the system. Figure 8 shows the evolution of the disk for that system. The evolution of the radial velocity dispersion is shown in figure 9. Essentially the same result is obtained, as illustrated in figure 6, with very little increase in σ_r for the spherical stars and sizable increases for the point stars. Note that in the region $r < 2$ kpc, the epicyclic frequency corresponding to the fixed component of the field is constant and σ_r remains at a very small value.

CONCLUDING REMARKS

Since collisional and numerical relaxation effects have been shown to be negligible, the heating occurring in disk galaxy models is caused by collective or violent relaxation. The results presented here show that the heating and the associated short-wavelength unstable modes can be effectively suppressed by using the interaction potential corresponding to uniform-density spherical stars rather than that of point stars. Thus, for the study of large-scale galactic stability, or large-scale density wave propagation, the use of an interaction potential corresponding to a uniform-density spherical star will be desirable since collective heating effects would no longer mask the phenomena under study.

Langley Research Center,
National Aeronautics and Space Administration,
Hampton, Va., February 12, 1974.

REFERENCES

1. Hohl, F.: Relaxation Time in Disk Galaxy Simulations. Astrophys. J., vol. 184, no. 2, pt. 1, Sept. 1, 1973, pp. 353-359.

2. Miller, R. H.; Prendergast, K. H.; and Quirk, William J.: Numerical Experiments on Spiral Structure. Astrophys. J., vol. 161, no. 3, pt. 1, Sept. 1970, pp. 903-916.

3. Hohl, Frank: Numerical Experiments With a Disk of Stars. Astrophys. J., vol. 168, pt. 1, Sept. 15, 1971, pp. 343-359.

4. Lynden-Bell, D.: Statistical Mechanics of Violent Relaxation in Stellar Systems. Mon. Notic. Roy. Astron. Soc., vol. 136, no. 1, 1967, pp. 101-121.

5. Toomre, Alar: On the Gravitational Stability of a Disk of Stars. Astrophys. J., vol. 139, no. 4, May 15, 1964, pp. 1217-1238.

6. Hohl, Frank: Evolution of a Stationary Disk of Stars. J. Comput. Phys., vol. 9, no. 1, Feb. 1972, pp. 10-25.

7. Hohl, Frank: Dynamical Evolution of Disk Galaxies. NASA TR R-343, 1970.

8. Schmidt, Maarten: Rotation Parameters and Distribution of Mass in the Galaxy. Galactic Structure, Adriaan Blaauw and Maarten Schmidt, eds., Univ. of Chicago Press, c.1965, pp. 513-530.

9. Lin, C. C.; Yuan, C.; and Shu, Frank H.: On the Spiral Structure of Disk Galaxies – III. Comparison With Observations. Astrophys. J., vol. 155, no. 3, pt. 1, Mar. 1969, pp. 721-746.

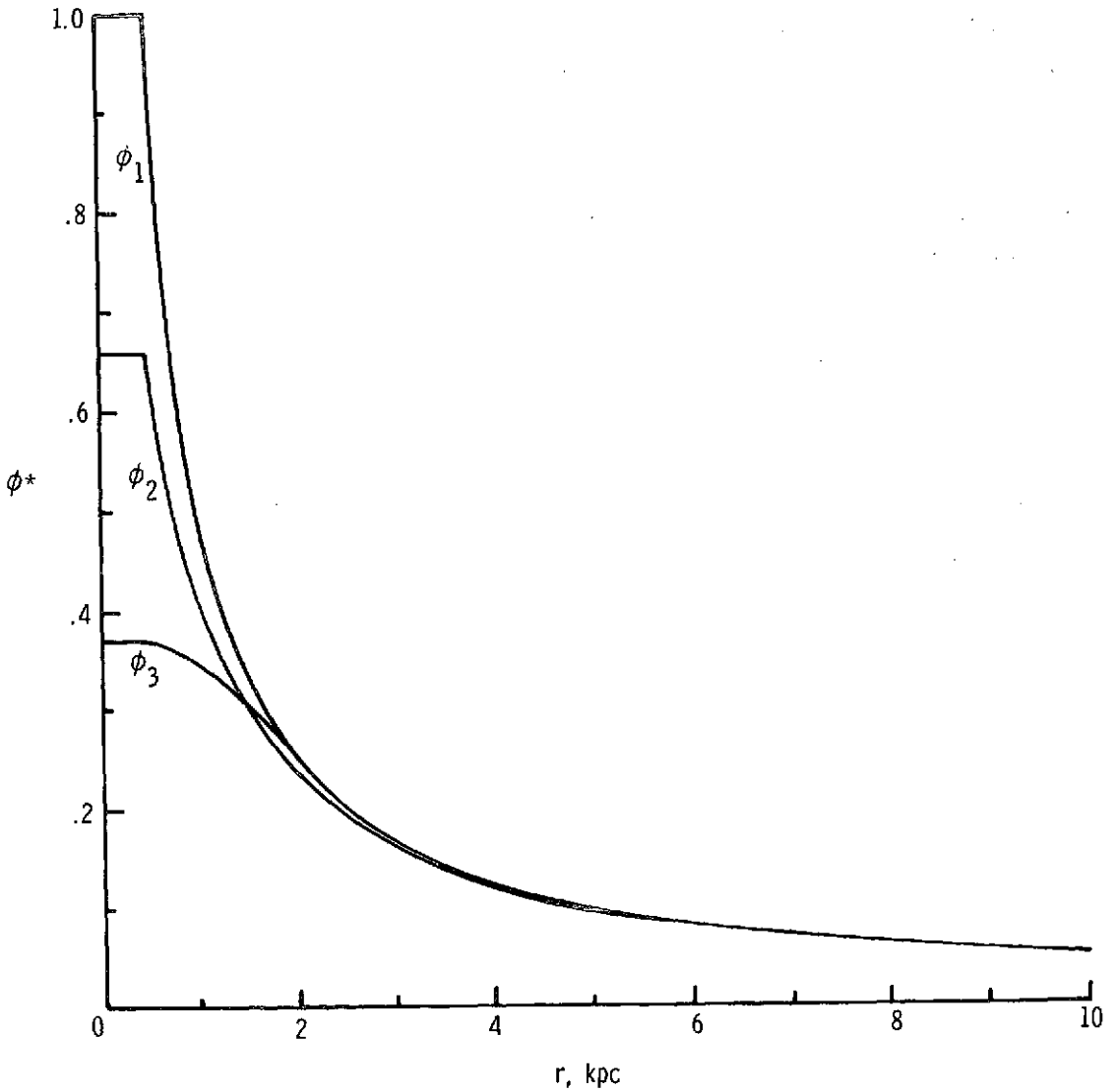

Figure 1.- Normalized interaction potential $\left(\phi^* = \frac{\phi}{2Gm}\right)$ for point stars (ϕ_1), rod stars of length 2 kpc (ϕ_2), and uniform-density spherical stars of radius 2 kpc (ϕ_3).

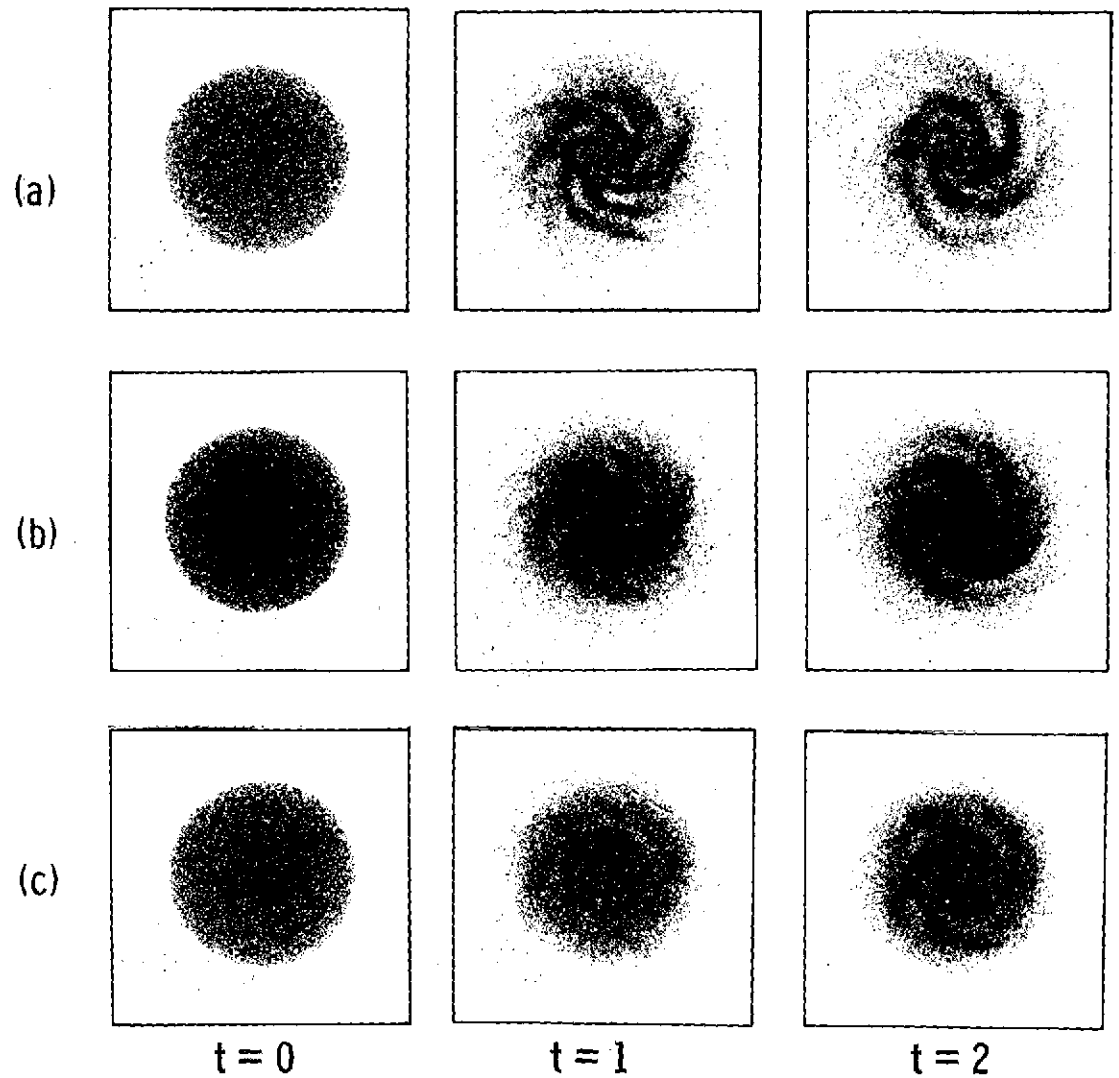

(a) Point stars.
(b) Mass rods of length 2 kpc.
(c) Spherical stars of radius 2 kpc.

Figure 2.- Evolution of a disk of 50 000 mutually interacting stars under the influence of a radial gravitational field similar to the Schmidt model of the galaxy. The stars contain 20 percent of the total mass of the galaxy. The initial velocity dispersions are such that Toomre's local criterion for axisymmetric stability is satisfied. Time shown is in units of the rotation period at $r = 10$ kpc.

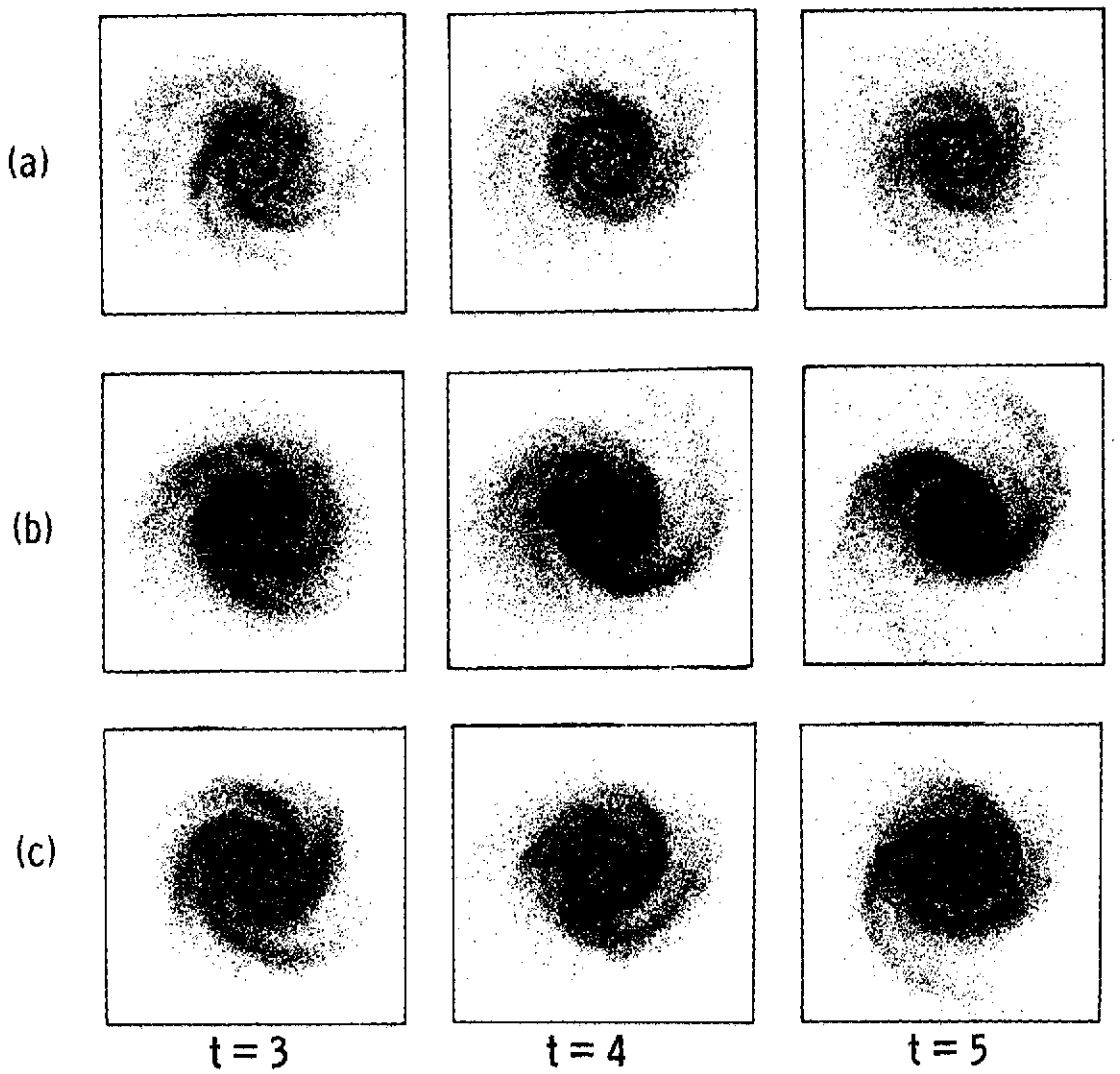

Figure 2.- Concluded.

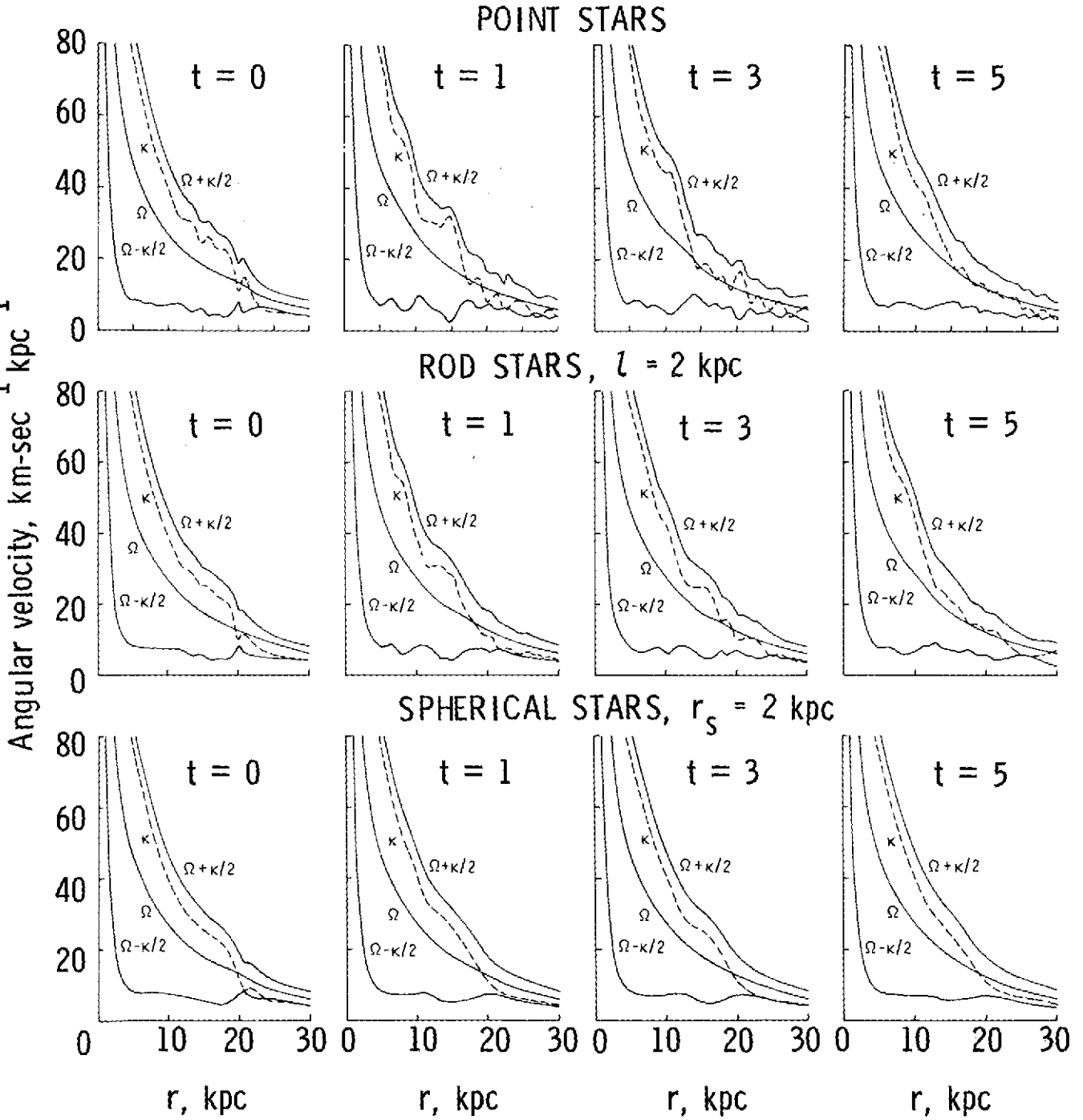

Figure 3.- Rotation curve, epicyclic frequency, and so forth of the simulated disk galaxies.

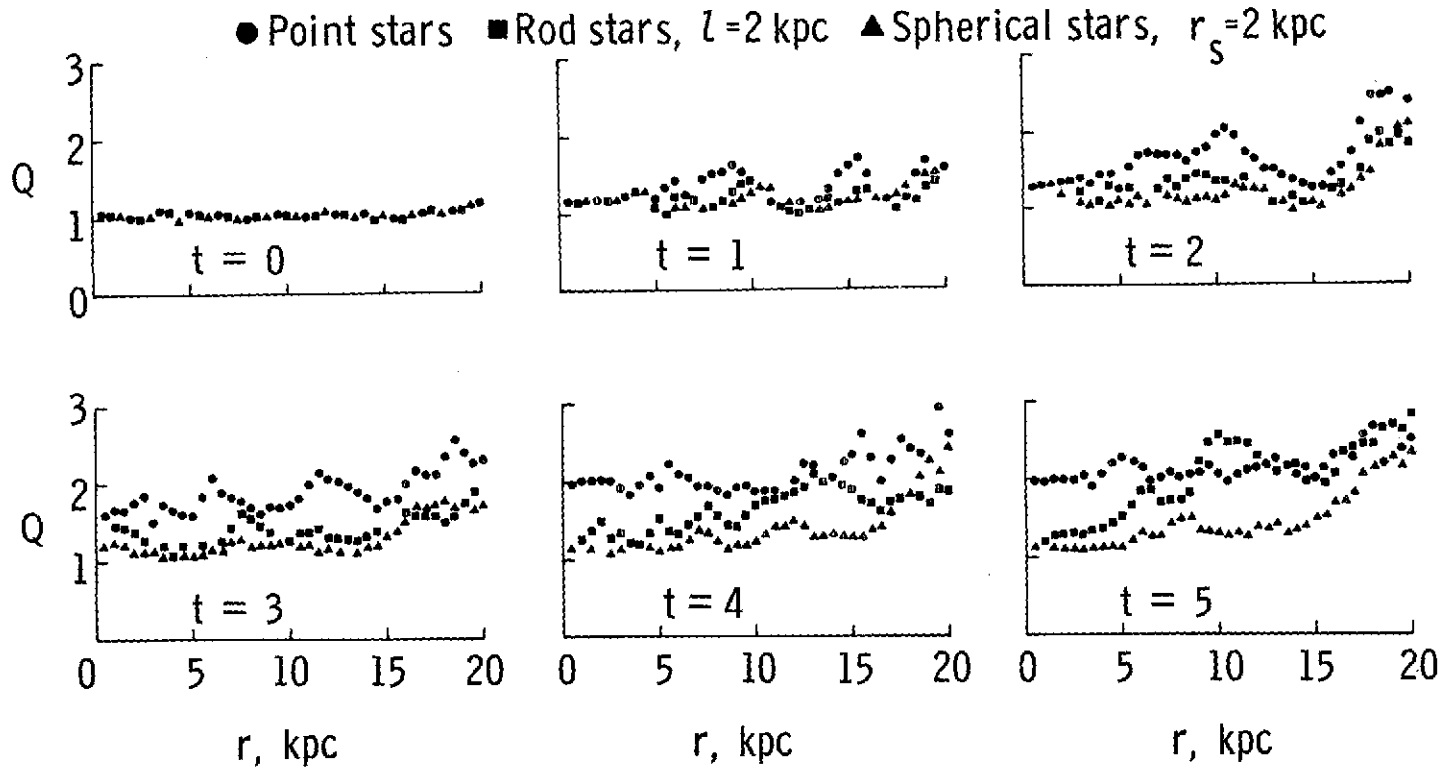

Figure 4.- Evolution of $Q = \frac{\sigma_r}{\sigma_{r,min}}$ for the three interaction potentials.

Note the low heating rate for spherical stars.

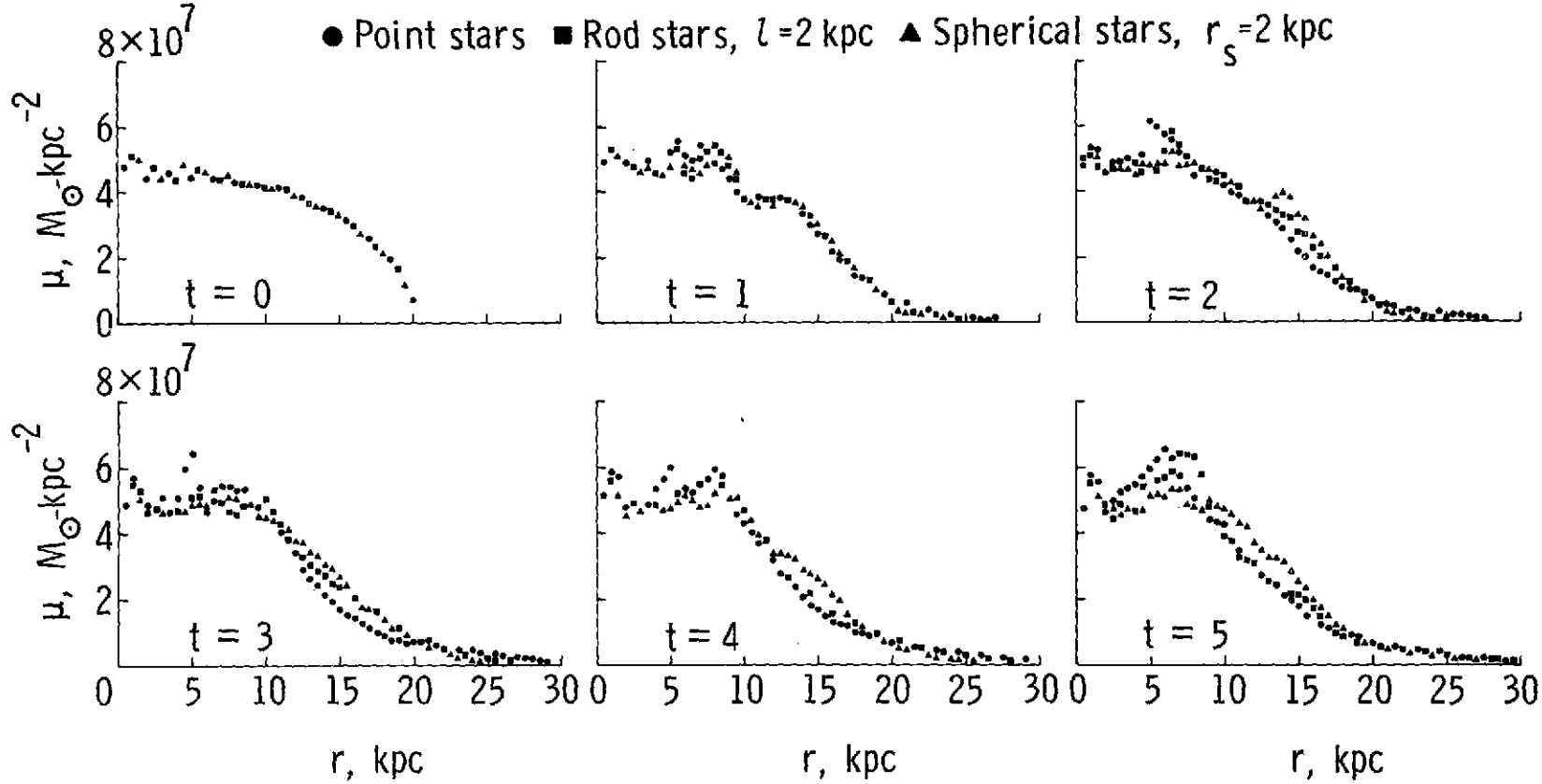

Figure 5.- Evolution of the axisymmetrically averaged surface mass density. There is a considerable reduction in the mass density in the region from 10 to 15 kpc during the evolution of the disk.

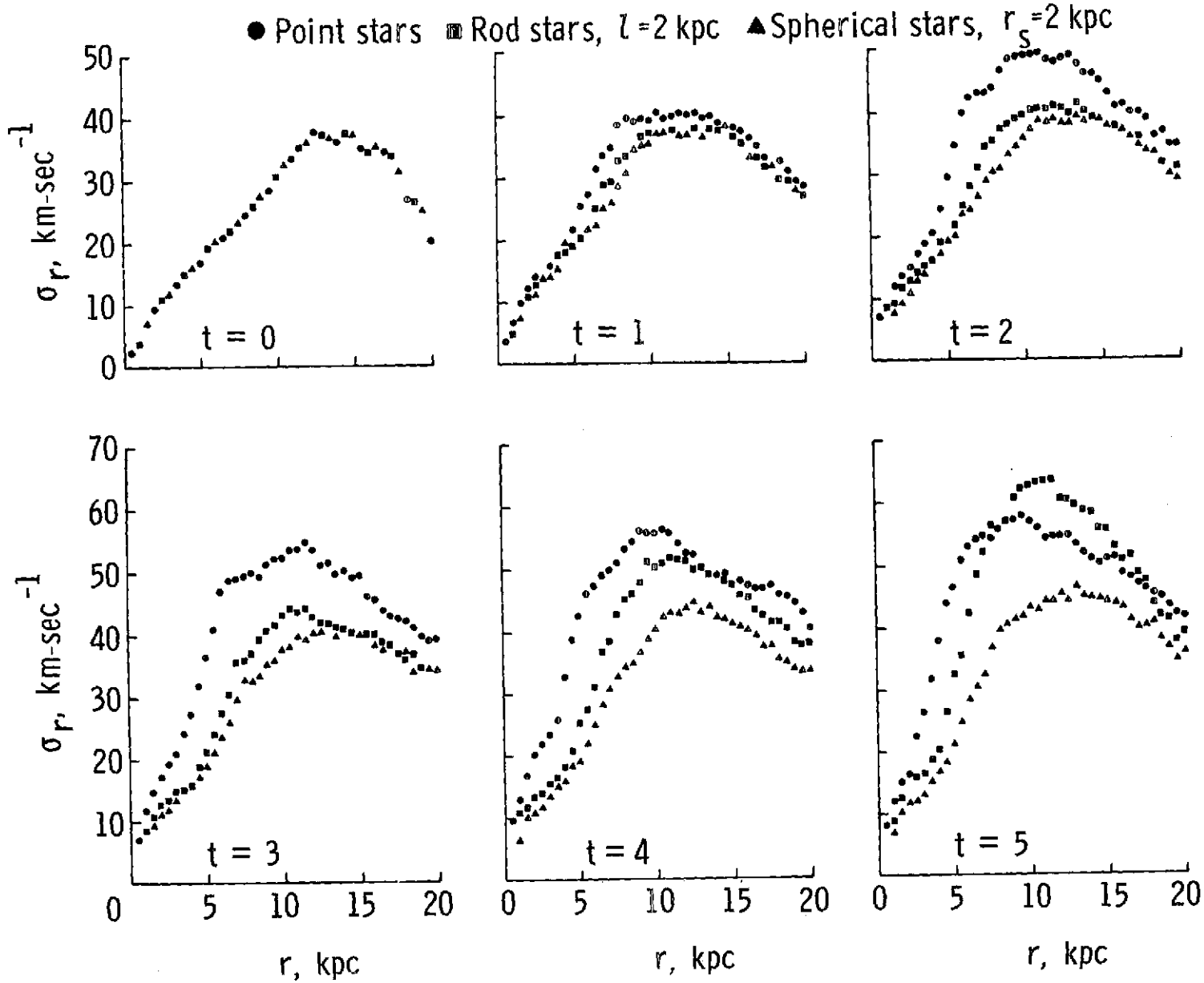

Figure 6.- Time history of the radial velocity dispersion.

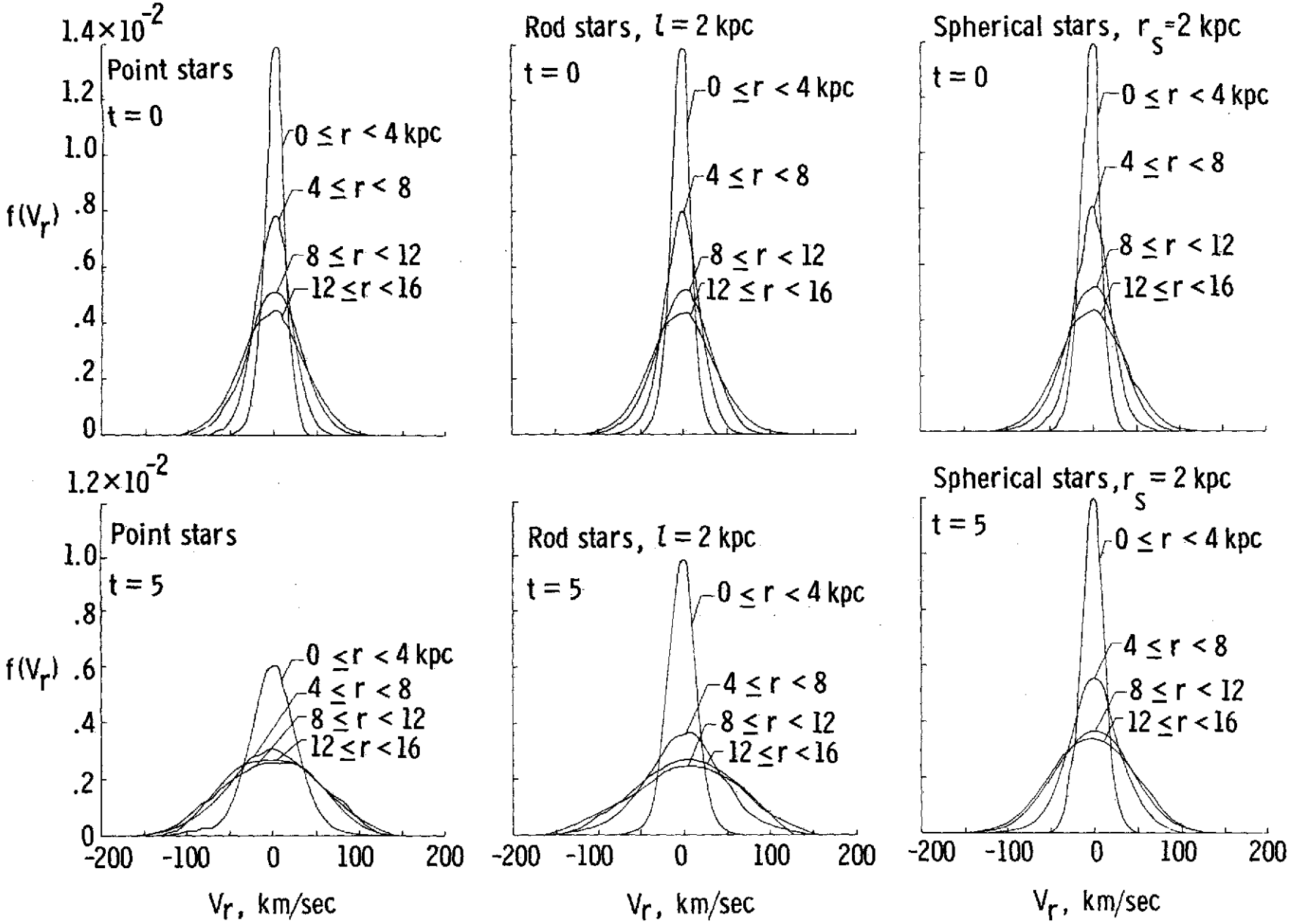

Figure 7.- Evolution of the radial velocity distribution for stars in various regions of the disk.

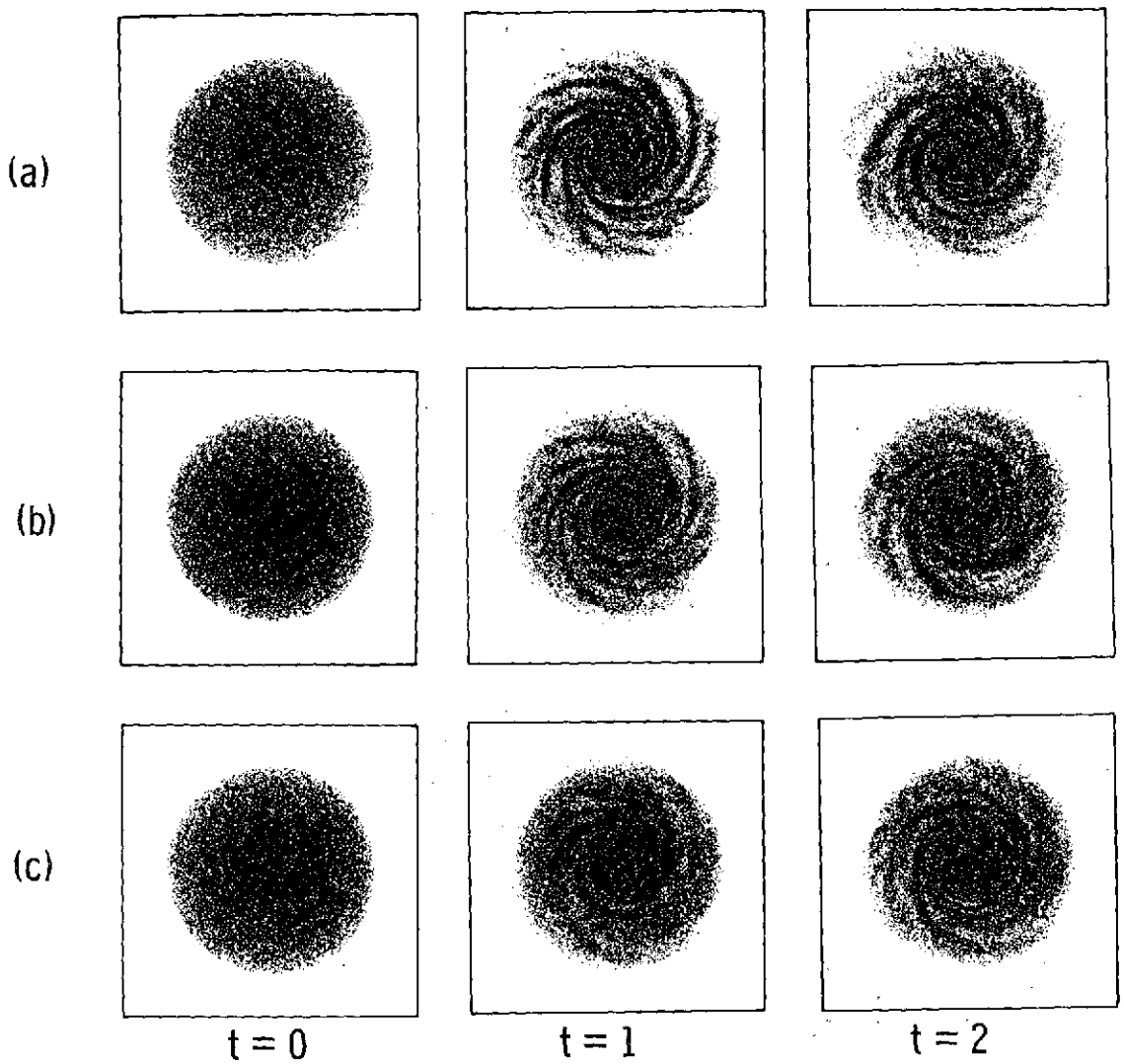

(a) Point stars.
(b) Mass rods of length 2 kpc.
(c) Spherical stars of radius 2 kpc.

Figure 8.- Evolution of a disk of 50 000 stars under the influence of a fixed field corresponding to a uniform-density spherical mass of radius 2 kpc. The stars contain 10 percent of the total mass of the galaxy.

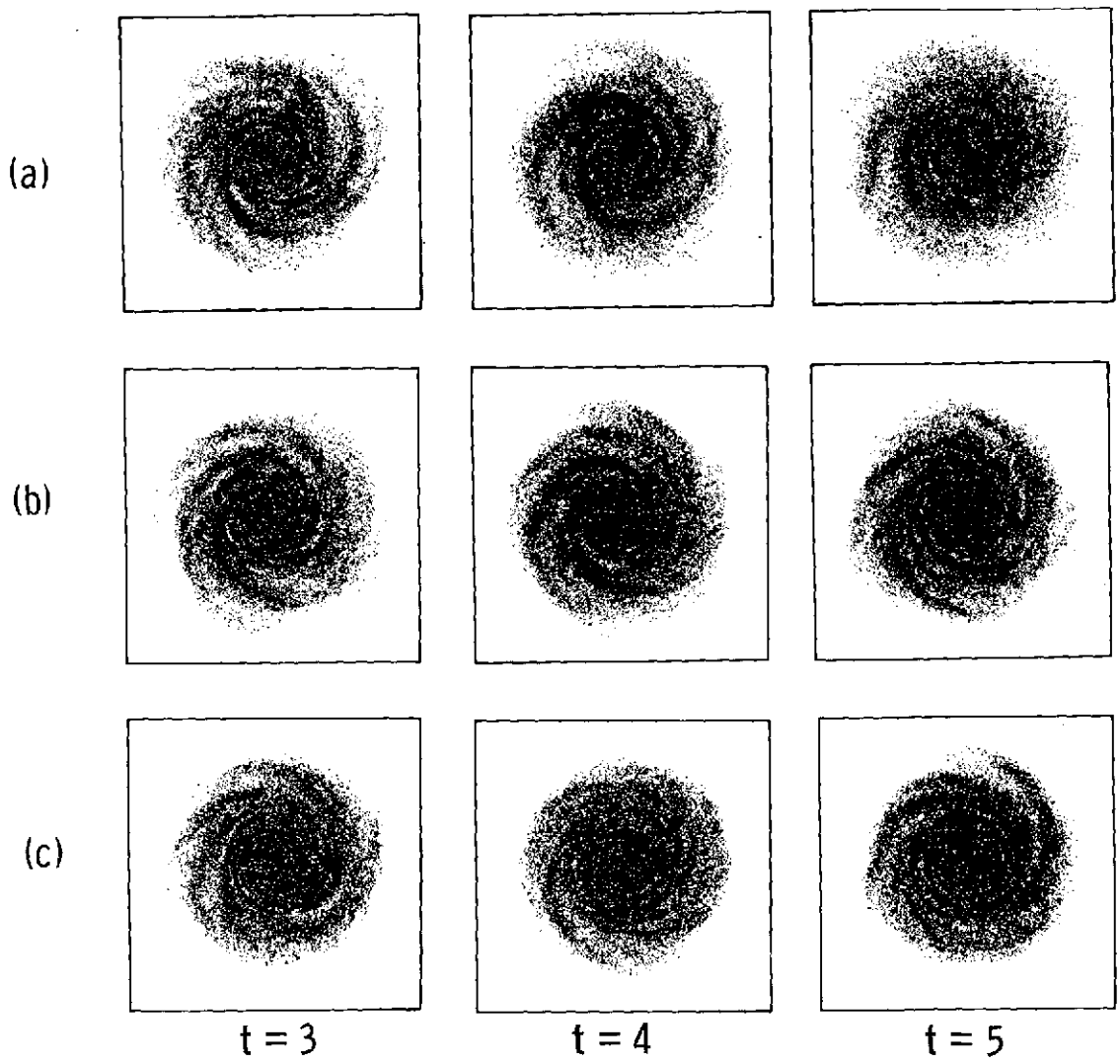

Figure 8.- Concluded.

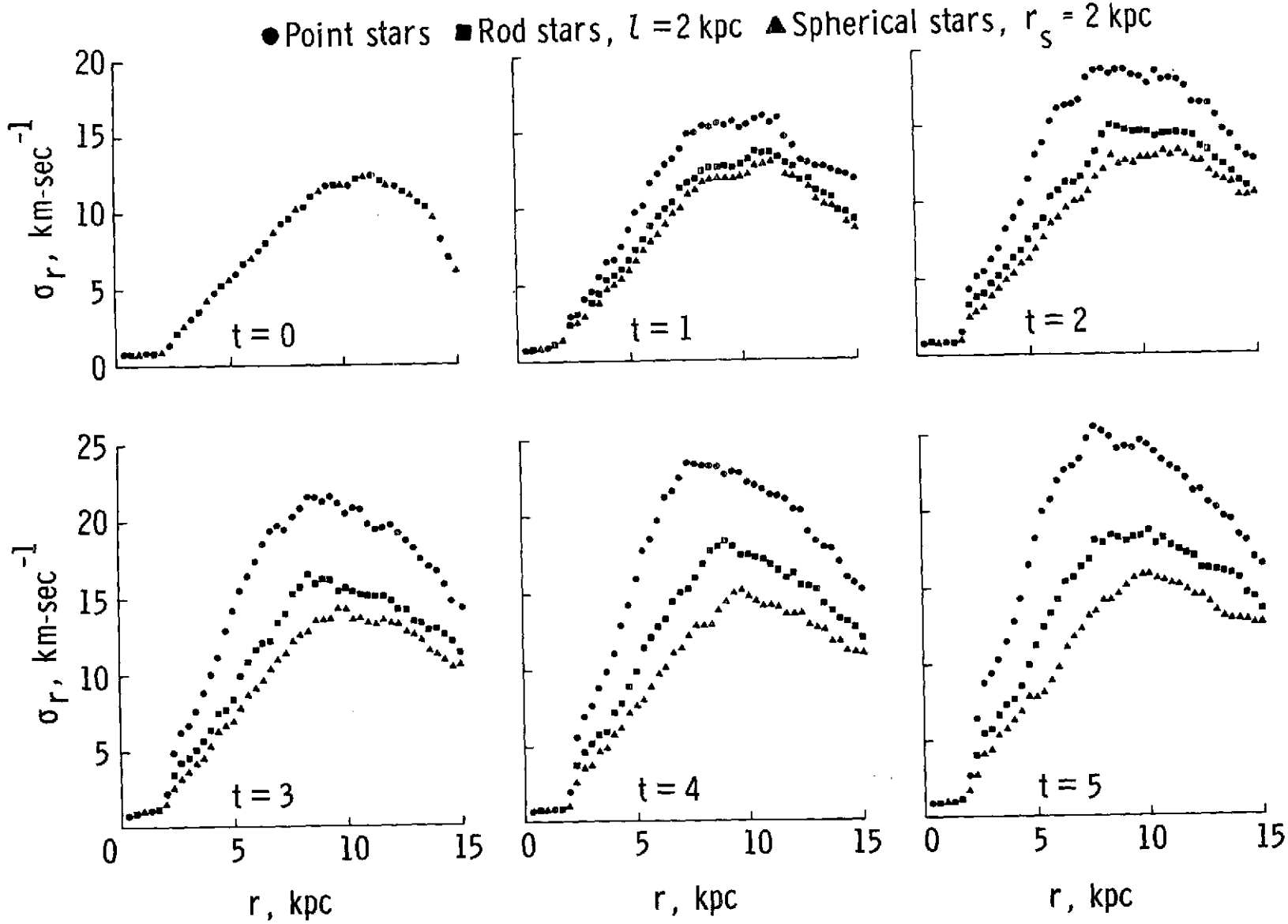

Figure 9.- Time history of the radial velocity dispersion for the system shown in figure 8.